Available online at www.sciencedirect.com
ScienceDirect
Ceramics International 38S (2012) S635–S639
CERAMICS INTERNATIONAL
www.elsevier.com/locate/ceramint

Synthesis and growth model of silicon oxide nanorods with bud-like structures

C.W. Zhou, K.F. Cai *

Functional Materials Research Laboratory, Tongji University, Shanghai 200092, China

Available online 27 May 2011

Abstract

A simple route was developed to synthesize amorphous silicon oxide nanorods with bud-like structures on Si (1 1 1) wafers, using $SiCl_4$ as Si source and Au as catalyst in a flowing H_2–5% Ar atmosphere, without using template and any additive. The nanostructures were characterized using field-emission scanning electron microscopy, transmission electron microscopy equipped with energy dispersive X-ray spectroscopy. Each silicon oxide nanorod with a bud-like structure at its tip has smooth surface and uniform diameter. The growth of the silicon oxide nanostructures may follow Solid–Vapor–Liquid–Solid and Vapor–Liquid–Solid mechanisms.

Keywords: C. Optical properties; D. SiO_2; CVD; Nanorods

1. Introduction

The fabrication of one-dimensional (1D) nanostructures, such as nanowires [1], nanorods [2], nanotubes [3], nanobelts [4], has attracted great attention due to their novel physical properties and potential application in nanoelectronic and optoelectronic devices, such as diodes, transistors, Josephson junctions, high-resolution optical heads of scanning near-field optical microscopes, localization of light, optical communications, sensors, and especially for nano-interconnection in future [5]. Among 1D nanomaterials, 1D silicon oxide nanostructures have recently attracted tremendous attention mainly due to their strong blue photoluminescence and possible application in integrated optics [6]. Moreover, silicon oxide nanowires (SONs) have been reported to emit red, green and ultraviolet light [7].

Several fabrication routes to silicon oxide nanostructures have been developed. For example, Lai et al. [7] used rapid thermal annealing process and Pt catalyst to obtain SONs. Kim et al. [6] prepared SONs during carbonization of polyimide thin film on the Si substrate. Yun et al. [8] synthesized SONs on organic polymer substrates by the help of plasma-enhanced chemical vapor deposition method. Chen and Ruoff [9] utilized high temperature without catalyst to fabricate SONs under flowing Ar–H_2 mixture gas. Kim et al. [10] prepared SONs on Pd-coated Si substrates by heat treatment at high temperature. The growth of the SONs usually depends on one kind of mechanism, such as oxide-assisted growth, vapor–liquid–solid (VLS), solid–vapor–liquid–solid (SVLS) [11] or solid–liquid–solid (SLS) [12] mechanism. Few reports can be found on the growth of silicon oxide nanostructures related to two or more mechanisms.

In this paper, we reported a simple metal-catalyzed CVD method for the growth of bud-like silicon oxide nanostructures on Au-coated Si (1 1 1) substrates. The growth mechanism for the nanostructures was discussed.

2. Experimental

One-side-polished Si (1 1 1) wafers (n-type, ρ = 25–30 Ω-cm) were used as substrates after being cleaned by conventional method. A 5-nm thick Au layer was thermally deposited on the substrates. The Au-coated substrate was placed on a corundum plate, and then transferred into a long quartz-tube system (see Fig. 1). The system was evacuated by a mechanical pump, flushed with Ar gas for once or ten times, and then Ar gas was kept flowing into the tube at a rate of 100 ml/min. When the furnace temperature reached 1000 °C, the Ar gas was switched

* Corresponding author. Tel.: +86 21 65980255; fax: +86 21 65980255.
E-mail address: kfcai@tongji.edu.cn (K.F. Cai).

0272-8842/$36.00
doi:10.1016/j.ceramint.2011.05.115

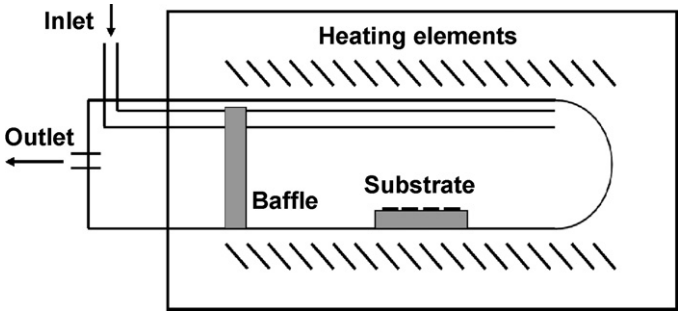

Fig. 1. Schematic diagram of the main part of the quartz tube system.

to H_2–5% Ar gas (∼100 ml/min) and the system was gradually inserted into the furnace. When the furnace temperature was stable at 1000 °C again, another stream of H_2–5% Ar gas with a flow rate of ∼20 ml/min was switched on as carrier gas and passed through a sealed glass container filled with liquid $SiCl_4$ (Alfa Aesar), which was immersed in an ice-water bath, to carry $SiCl_4$ vapor into the reaction zone for 10 or 15 min. After that, the carrier gas and furnace were turned off, and the furnace was cooled naturally to room temperature with a H_2–5% Ar flow (∼20 ml/min).

Products grown on the substrates were examined by field emission scanning electron microscopy (FESEM, Quanta 200 FEG) and transmission electron microscopy (TEM, Hitachi,

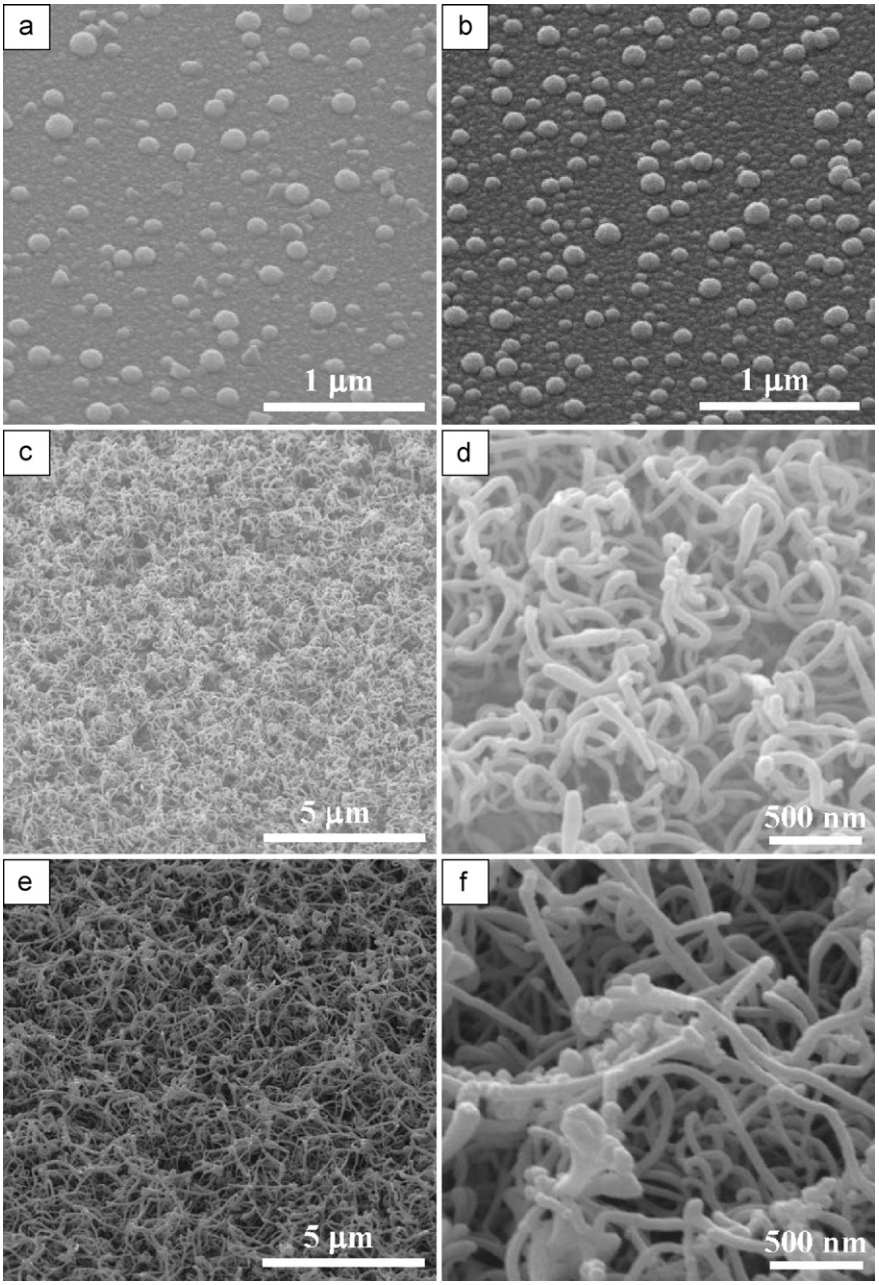

Fig. 2. FESEM images of samples (a) S_{1-10}; (b) S_{1-15}; (c) and (d) S_{10-10}; (e) and (f) S_{10-15}; (d) and (f) high-magnification FESEM images of the local areas in (c) and (e), respectively.

H-800 & FEI, S-TWIN 20) equipped with energy dispersive X-ray spectroscopy (EDX, EDAX).

3. Results and discussion

Fig. 2 shows the FESEM images of the samples synthesized under different conditions. For simplicity, the samples are named as S_{m-n}, where m and n stand for Ar-flushing times and duration time (in minute) for introducing the $SiCl_4$ vapor, respectively. Besides several pits, most surfaces of the samples S_{1-10} and S_{1-15} are covered with nanoparticles. The diameter of the nanoparticles ranges from ~80 to 180 nm (see Fig. 2a and b). Around the pits, 1D nanostructures can be observed under FESEM, which will be described hereinafter (see Fig. 4). The nanoparticles consist of Au, Si and O determined by EDX analyses. It can be seen from Fig. 2a and b that the amount of nanoparticles increases with the increasing of duration time for introducing the $SiCl_4$ vapor. Fig. 2c and e show the FESEM images of the samples S_{10-10} and S_{10-15}, respectively. The corresponding high-magnification images (Fig. 2d and f, respectively) clearly show the characteristic of the nanostructures. Numerous 1D nanostructures formed when the Ar-flushing times changed from once to 10 times. Sample S_{10-10} consists of bunches of nanorods. The nanorods are ~40–95 nm in diameter and not shorter than 740 nm. Sample S_{10-15} also consists of bunches of nanorods. But each nanorod has a bud-like structure at its tip. The nanorods are ~35–80 nm in diameter and not shorter than 1.5 μm. The above results indicate that both the Ar-flushing times and the duration time for introducing the $SiCl_4$ vapor have significant effects on the morphology of the samples.

Fig. 3a shows a typical TEM image of the nanorods (marked by A, B and C) corresponding to sample S_{10-15}. The nanorods are smooth and relatively uniform (~15–35 nm in diameter). Each nanorod in Fig. 3a has a black nanostructure at one end. The composition of the black nanostructure is different from the nanorod owing to different contrasts. Selected area electron diffraction (SAED) analysis (not shown here) reveals that the black nanostructures and the nanorods are single crystal and amorphous, respectively. EDX analysis indicates that the nanorods consist of Si and O and that the black nanostructures consist of Au (see Fig. 3c and d). By combining SAED and EDX results, it can be speculated that the black nanostructure is single crystal Au and the nanorods amorphous SiO_x ($1.5 < x < 2$, due to O/Si atomic ratio close to 2). C and Cu signals in the spectra are from TEM sample holders (C signal in Fig. 3c is relatively weak due to the shielding effect of the big and thick Au-containing head). These imply that the growth of the nanorods is catalyzed by the Au nanostructures. Usually, catalyst particle for 1D nanostructures growth is spherical. The black Au nanostructures in the present work are cylindrical (see A in Fig. 3a) and irregular (see B and C in Fig. 3a), similar to that reported in ref. [7]. From the morphology of the three nanorods with different-shape Au particles, we deduce that they represent three growth stages of the silicon oxide nanorods. The sequence is A, B, and C. Especially, C nanorod clearly has a

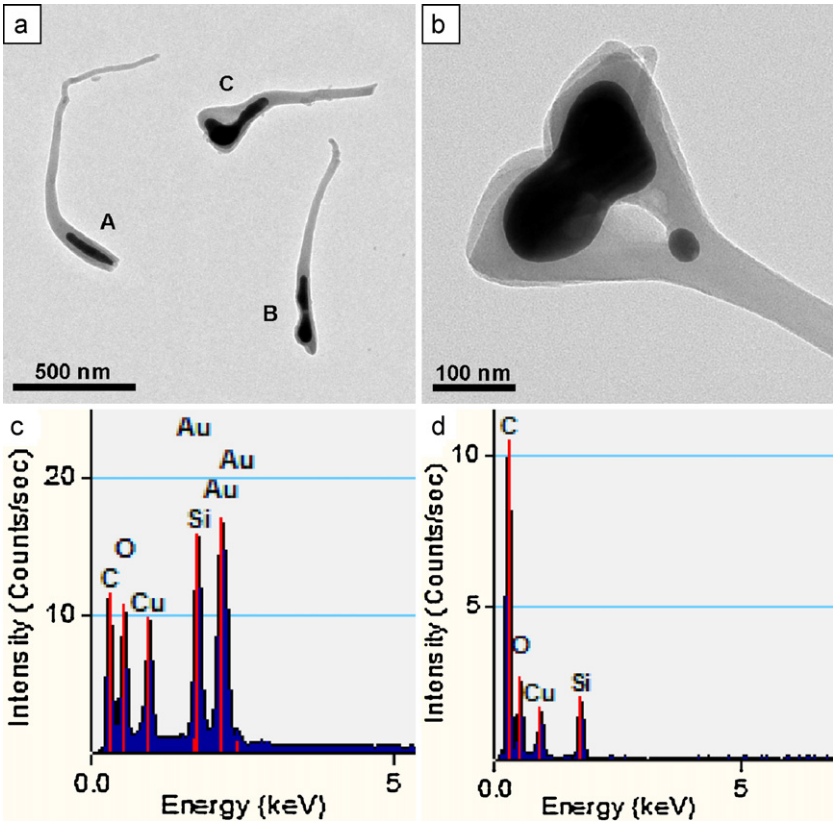

Fig. 3. (a) and (b) TEM images of sample S_{10-15}; (c) and (d) typical EDX spectra recorded on the black nanostructure and rod part of the nanorods, respectively.

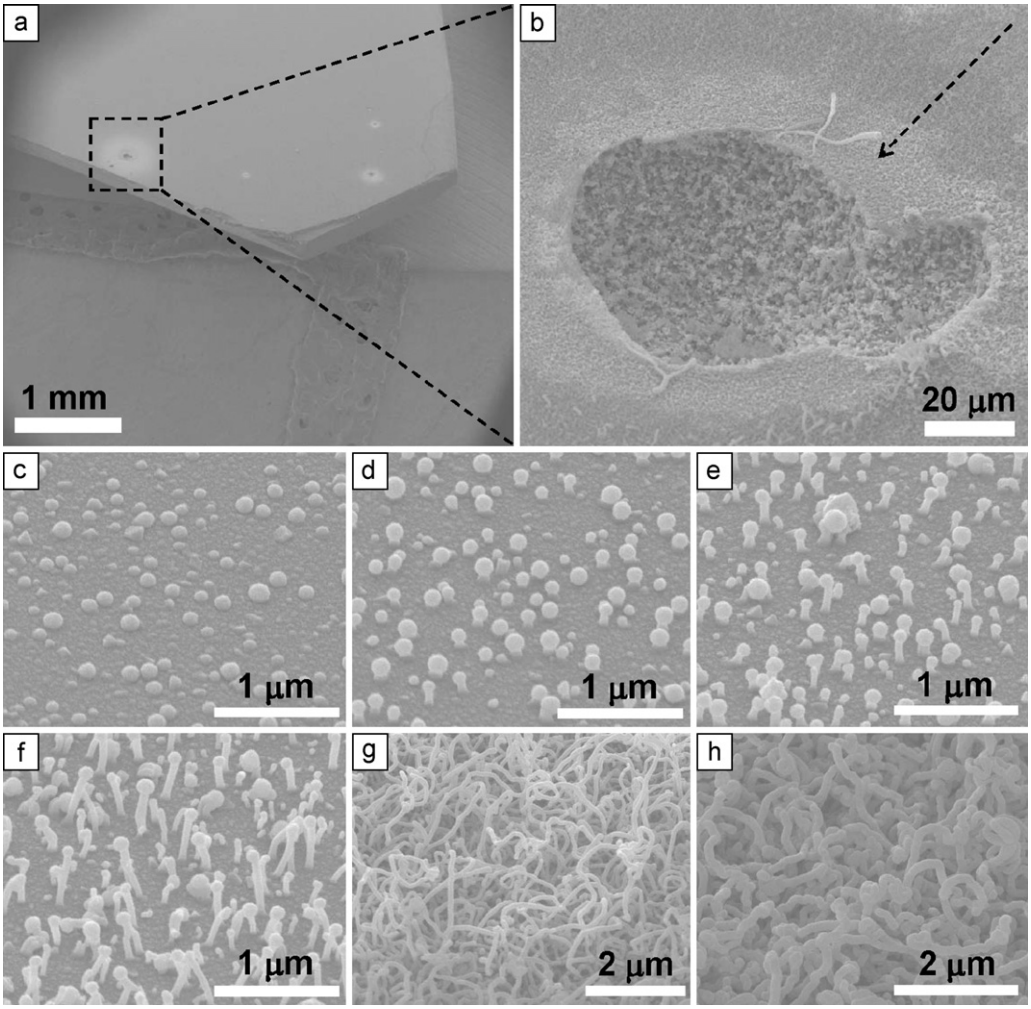

Fig. 4. FESEM images of sample $S_{1–10}$: (a) FESEM image of the growth surface of the Si substrate; (b) high-magnification FESEM image of one pit marked in (a); (c)–(h) FESEM images of the area around the pit along the direction indicated by the arrow in (b).

bud-like structure at its tip, and its Au nanoparticle has a shape similar to its bud. Fig. 3b is a TEM image corresponding to sample $S_{10–15}$, which shows another nanorod with a bud-like structure. The nanorod has ∼60 nm in diameter. It is of interest to note that the Au nanostructure of the nanorod consist of two parts: one is big, irregular and located at the tip of the bud, and the other is small, spherical and located at the junction between the rod and the ''bud''. It is deduced from the characteristic of the Au particles in Fig. 3a and b that the Au particle plays an important role in the formation of the bud-like structure. As the Au catalysts shown as in Fig. 3a and b are not in stable shapes (spherical is more stable), we further deduce that if the duration time for introducing the $SiCl_4$ vapor is prolonged, the bud-like nanostructure will develop into another nanostructure, which is under progress in our group.

Fig. 4a shows a low-magnification FESEM image of sample $S_{1–10}$. Several pits can be observed on the substrate. Fig. 4b shows the high-magnification FESEM image of the pit marked in Fig. 4a. Fig. 4c–h show the FESEM images of different zones around the pit along the direction indicated by the arrow in Fig. 4b. A clear growth process of the nanostructures can be seen from this series images. Combining these results with that reported in ref. [13], it can be deduced that the Si substrate can supply Si species at high temperatures. Therefore, the growth for the bud-like nanostructures is related to SLS and/or SVLS mechanism. The growth of the bud-like nanostructures is proposed as follows.

As the temperature increases and above the Au–Si eutectic point (∼363 °C), the Au from the film and the Si from the substrate slowly form Au–Si alloy liquid. And as the temperature further increases, more Au–Si alloy liquid forms and finally shrinks to form Au–Si droplets. At the same time the Si substrate is etched by the hot droplets to create Si species around the Au–Si alloy droplets. The droplets serve as preferential sites for absorption of the Si species and oxygen, which may come from the residual oxygen and the H_2–5% Ar gas [13]. Therefore, finally, Au–Si–O alloy droplets form [11]. As the temperature increases to 1000 °C (but not enough Si species from the $SiCl_4$ vapor), the concentration of Si and O in the droplet increases and the Si and O react to form silicon oxide. And when the solution becomes supersaturated with the silicon oxide species, silicon oxide will precipitate from the solution to form silicon oxide nanoparticles on the lower hemispherical surface of the droplet. These nanoparticles act as

nucleation sites, initiating the growth of the silicon oxide nanorods. At this stage, Si source almost comes from the Si substrate so the growth mechanisms are SLS and SVLS mechanisms. Of course, once the droplet is lifted up by the nanorod and loses contact with the substrate, the Si species cannot diffuse anymore from the substrate into the droplet so SVLS mechanism will dominate the growth of the silicon oxide nanorods. As the $SiCl_4$ vapor starts to supply Si species, the silicon oxide nanorods grow faster so that the growth mechanism at this stage includes SVLS and VLS, but the latter dominates. Because of the baffle in our special reaction chamber (Fig. 1), the concentration of the Si species in the system increases dramatically. The higher concentration leads to more easy-to-produce nucleation sites at the connect part between the alloy droplet and silicon oxide nanorod. These sites absorbing the reactants naturally expand the head of the nanorod so that the bud-like structure forms. During the expanding and growing up, the catalytic droplet inevitably transforms. The growth at this stage is mainly controlled by VLS mechanism. When the carrier gas and the furnace are turned off, the reaction is stopped so that the state of the droplet is reserved, as shown in Fig. 3a and b.

As the silicon oxide nanostructures grow too fast for the atoms to stack into crystalline order and the temperature is not high enough to allow recrystallization of the atomic Si–O species, the products are amorphous.

The reason why multiple Ar-flushing is beneficial to the growth of the silicon oxide nanostructures is not yet clear, which needs to be further studied.

4. Conclusions

Amorphous silicon oxide nanorods with bud-like structures have been synthesized via a Au-catalyzed CVD method using a simple device. The nanorods are ∼15–95 nm in diameter and longer than 1 μm. The growth of the nanorods may follow SLS and SVLS mechanisms at the early stage and both SVLS and VLS mechanisms at later stage. The SiO_x nanorods with bud-like nanostructures may find particular applications in future, such as novel optoelectronic nanodevices.

Acknowledgement

This work is financially supported by the National Natural Science Foundation of China (50872095).

References

[1] D.J. Gargas, M.E. Toimil-Molares, P.D. Yang, Imaging single ZnO vertical nanowire laser cavities using UV-laser scanning confocal microscopy, Journal of the American Chemical Society 131 (2009) 2125–2127.
[2] H. Zhu, J. Tao, X. Dong, Preparation and photoelectrochemical activity of Cr-doped TiO_2 nanorods with nanocavities, Journal of Physical Chemistry C 114 (2010) 2873–2879.
[3] X.H. Zhong, Y.L. Li, Y.K. Liu, X.H. Qiao, Y. Feng, J. Liang, J. Jin, L. Zhu, F. Hou, J.Y. Li, Continuous multilayered carbon nanotube yarns, Advanced Materials 22 (2010) 692–696.
[4] X.S. Fang, Y. Bando, M.Y. Liao, T.Y. Zhai, U.K. Gautam, L. Li, Y. Koide, D. Golberg, An efficient way to assemble ZnS nanobelts as ultraviolet-light sensors with enhanced photocurrent and stability, Advanced Functional Materials 20 (2010) 500–508.
[5] L.W. Lin, Y.H. Tang, C.S. Chen, Self-assembled silicon oxide nanojunctions, Nanotechnology 20 (2009) 175601.
[6] J.H. Kim, H.H. An, C.S. Yoon, Enhanced photoluminescence of silicon oxide nanowires brought by prolonged thermal treatment during growth, Journal of Applied Physics 105 (2009) 076102.
[7] Y.S. Lai, J.L. Wang, S.C. Liou, C.H. Tu, Size and density control of silicon oxide nanowires by rapid thermal annealing and their growth mechanism, Applied Physics a-Materials Science & Processing 94 (2009) 357–363.
[8] J. Yun, Y. Jeong, G.H. Lee, Direct synthesis of silicon oxide nanowires on organic polymer substrates, Nanotechnology 20 (2009) 365606.
[9] X.Q. Chen, R.S. Ruoff, Simple and catalyst-free synthesis of silicon oxide nanowires and nanocoils, Nano 2 (2007) 91–95.
[10] H.W. Kim, S.H. Shim, J.W. Lee, C. Lee, H.J. Hwang, S.Y. Chung, H.S. Kim, S.K. Hwang, G.Y. Yeom, N.E. Lee, J.B. Yoo, Y.C. Joo, H.J. Kim, E. Yoon, Synthesis, structural characterization and photoluminescence properties of SiO_x nanowires prepared using a palladium catalyst, Journal of the Korean Physical Society 50 (2007) 1799–1802.
[11] D Bahloul-Hourlier, P. Perrot, Thermodynamics of the Au-Si-O system: application to the synthesis and growth of silicon-silicon dioxide nanowires, Journal of Phase Equilibria and Diffusion 28 (2007) 150–157.
[12] H.F. Yan, Y.J. Xing, Q.L. Hang, D.P. Yu, Y.P. Wang, J. Xu, Z.H. Xi, S.Q. Feng, Growth of amorphous silicon nanowires via a solid-liquid-solid mechanism, Chemical Physics Letters 323 (2000) 224–228.
[13] Z.W. Pan, Z.R. Dai, C. Ma, Z.L. Wang, Molten gallium as a catalyst for the large-scale growth of highly aligned silica nanowires, Journal of the American Chemical Society 124 (2002) 1817–1822.